Nikola André Fitzen, Patricia Martínez Díaz, Olaf Dössel, and Axel Loewe*

Impact of the Right Atrium on Arrhythmia Vulnerability

https://doi.org/10.1515/cdbme-2023-1036

Abstract: Atrial fibrillation (AF) is one of the most common cardiac diseases. However, a complete understanding of how to treat patients suffering from AF is still not achieved. As the isolation of the pulmonary veins in the left atrium (LA) is the standard treatment for AF, the role of the right atrium (RA) in AF is rarely considered. We investigated the impact of including the RA on arrhythmia vulnerability in silico. We generated a dataset of five mono-atrial (LA) and five bi-atrial models with three different electrophysiological (EP) setups each, regarding different states of AF-induced remodelling. For every model, a pacing protocol was run to induce reentries from a set of stimulation points. The average share of inducing points across all EP setups was 0.0, 0.8 and 6.7 % for the mono-atrial scenario, 0.5, 27.3 and 37.9 % for the bi-atrial scenario. The increase in inducibility of LA stimulation points from mono- to bi-atrial scenario was 0.91 ± 2.03%, 34.55 ± 14.9 % and 44.2 ± 14.9 %, respectively. In this study, the RA had a marked impact on the results of the vulnerability assessment that needs to be further investigated.

Keywords: Arrhythmia vulnerability assessment, right atrium, electrophysiology simulation, reentry inducibility

1 Introduction

Atrial fibrillation (AF) is one of the most prevalent cardiac diseases, affecting millions of people worldwide. Despite extensive research in methodology and technology, success rates of standard treatments like pulmonary vein isolation (PVI) have improved only slightly pointing out the need for further investigation. Thus, significant conceptual or technological shifts may be required to develop more effective methods to lastingly terminate AF [15]. The left atrium (LA) plays a crucial role in the initiation and maintenance of arrhythmia with the pulmonary veins having a well-studied role in the onset of AF [9]. The cardiomyocytes on the pulmonary veins (PVs) differ from the atrial cells in that they have unique action potential characteristics making them more prone to arrhythmogenesis [7]. During PVI, the PVs are electrically isolated with radiofrequency catheter ablation to prevent them from triggering or sustaining AF. The RA also contributes to the development of AF. Its structures such as the appendage are involved in arrhythmogenesis [12]. Furthermore, it was shown that additional RA ablation can terminate AF [10]. Taking this into account, a more comprehensive assessment of both atria may be necessary to plan optimal ablation strategies.

In silico arrhythmia vulnerability assessment (AVA) quantifies the inducibility of arrhythmias of an atrial model [2] by identifying the number of points that can trigger a reentry. Using AVA, it is also possible to compare different scenarios and evaluate the impact of a specific set of parameters on arrhythmia vulnerability in a controlled and reproducible manner. While these assessment tools are used to identify optimal ablation targets [4] and gain momentum clinically [5], they mostly consider only the LA. We thus aim to evaluate the impact of the RA on arrhythmia vulnerability by assessing differences between left mono-atrial and bi-atrial scenarios.

2 Methods

We used imaging data from 5 subjects to obtain original bi-atrial geometries [11]. For each geometry, we created a bi-layer model with annotated anatomical regions and fiber orientation with the AugmentA software [3]. The bi-atrial models included the Bachmann bundle (BB) and three further inter-atrial connections. Additionally, from each subject, a mono-atrial model with only the LA was generated.

2.1 Electrophysiology

We considered three different electrical remodelling scenarios by scaling the ionic conductances of the Courtemanche-Ramirez-Nattel (CRN) model [8] between healthy myocytes (H) and two levels of persistent AF electrical remodelling (M and S) [13]. The AF-induced remodelling factors (see Table 1, last row) were applied at 0 %, 50 % and 100 % for the whole atria in the scenarios H, mild remodelling (M) and severe remodelling (S), respectively. To take into account electrical anatomical heterogeneity, for each scenario we modified the maximum conductances of selected ionic channels (see Table 1) as described in previous studies [11, 13]. The mon-

Nikola André Fitzen, Patricia Martínez Díaz, Olaf Dössel, Axel Loewe, Institute of Biomedical Engineering, Karlsruhe Institute of Technology (KIT), Fritz-Haber-Weg 1, Karlsruhe, Germany, e-mail: publications@ibt.kit.edu

Tab. 1: Factors applied relative to the original CRN model due to the anatomical heterogeneity and additional AF-induced remodelling for the S state (last row). Bold factors differ from normal myocardium conductances. The M state factors were obtained by linearly interpolating the AF-induced remodelling factors at 50 %.

	Applied factor on maximum conductance							
Atrial region	**GCaL**	**Gto**	**GKr**	**GKs**	**GK1**	**GKur**	**INaCa**	**Ileak**
RA / PM	1.0	1.0	1.0	1.0	1.0	1.0	1.0	1.0
CT	**1.67**	1.0	1.0	1.0	1.0	1.0	1.0	1.0
BB	**1.67**	1.0	1.0	1.0	1.0	1.0	1.0	1.0
TVR	**0.67**	**1.53**	**1.53**	1.0	1.0	1.0	1.0	1.0
MVR	**0.67**	**1.53**	**2.44**	1.0	1.0	1.0	1.0	1.0
RAA	**1.06**	**0.68**	1.0	1.0	1.0	1.0	1.0	1.0
LAA	**1.06**	**0.68**	**1.6**	1.0	1.0	1.0	1.0	1.0
LA	1.0	1.0	**1.6**	1.0	1.0	1.0	1.0	1.0
PV	**0.75**	**0.75**	**2.4**	**1.87**	**0.67**	1.0	1.0	1.0
AF-induced remodelling	**0.45**	**0.35**	1.0	**2.0**	**2.0**	**0.5**	**1.6**	**1.5**

odomain tissue conductivities in longitudinal direction were tuned [16] to yield a conduction velocity (CV) of 1.2, 1.0 and 0.8 m/s along fiber direction for the scenarios H, M and S, respectively. The anisotropy ratios and propagation differences due to anatomical heterogeneity were modeled as in previous studies [13]. In total, we generated a set of ten atrial geometries, 5 bi-atrial and 5 LA mono-atrial, combined with the three EP states (H, M, S), leading to 30 different scenarios in total. The electrical propagation in the atria was simulated in openCARP by solving the monodomain equation [14, 16].

2.2 Arrhythmia Vulnerability Assessment

To assess arrhythmia vulnerability in each scenario, we ran the pacing at the end of the effective refractory period (PEERP) protocol with an inter-point distance of 2 cm as described in [2]. Briefly, from each stimulation point, a S1-S2 protocol was performed to induce a reentrant arrhythmia. Each model was initialized to a limit cycle in a single cell environment and then prepaced four times with a basic cycle length of 500 ms in tissue. For the mono-atrial models, the node with the earliest activation on the LA in the corresponding bi-atrial model was chosen as the first activation site. The PEERP protocol yielded a subset of the original stimulation points from which reentries were induced. The results were evaluated by comparing the share of inducing points to stimulation points. In addition, we classified reentries that were sustained for > 1 s as either AF or atrial flutter (AFlut) based on the tachycardia cycle length (TCL, 160 ms cutoff) and the presence of multiple wavefronts. As the same induction point can cause an arrhythmia that triggers, for example, AF in one atrium and AFlut in another, for the arrhythmia classification of the same inducing point we additionally defined 2 reference points, one in the posterior wall of the RA and the other in the posterior wall of the LA.

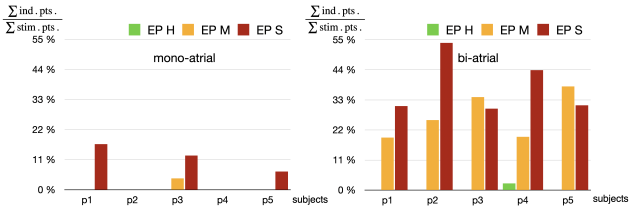

Fig. 1: Ratio of inducing points (ind. pts.) to stimulation points (stim. pts.) for the mono LA scenario (left) and the bi-atrial scenario (right), with each EP state plotted separately.

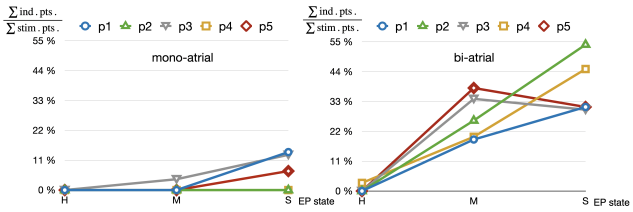

Fig. 2: Ratio of inducing points to stimulation points in relation to EP state for the mono LA scenario (left) and the bi-atrial scenario (right).

3 Results

The ratio of inducing points to stimulation points for each subject is shown in Figure 1 and 2. The average ratio in the mono-atrial scenario was 0.83 ± 1.86 % in the M and 7.17 ± 7.44 % in the S state. In the bi-atrial scenario for the sames states the average ratio was 27.27 ± 8.47 % and 37.87 ± 10.65 %. Only for the cases of subjects p3 and p5 in the bi-atrial scenario, more reentries were induced in the M than in the S state. The inclusion of the RA led to 34.6 ± 14.9 % and $44.4 \pm$ %14.8 % more inducing points in the LA in the M and S state, respectively (Figure 3). From the induced reentries in the mono-atrial scenario, 0 % in the M and 100 % in the S state were classified as AF. In the bi-atrial scenario 6.5 ± 9.29 % and 83.37 ± 18.59 % were classified as AF in at least one atrium in the M and S state, respectively. The ratio of AF classified reentries to inducing points varied between subjects (see Figure 4).

4 Discussion

We created a set of 30 simulation setups based on mono-atrial and bi-atrial imaging data and three different EP scenarios for 5 different subjects. For each subject, we compared the number of inducing points as well as the type of arrhythmias between the mono-atrial LA scenario and the corresponding bi-atrial scenario. We found that the inclusion of the RA leads to a marked increase in the share of inducing points. In the mono-atrial scenarios, no reentries were induced in the H scenarios

and in particular for subjects p2 and p4, no point was able to induce a reentry (see Figure 1, left). In general, we observed a consistently lower share of inducing points when compared to the corresponding bi-atrial scenarios. When evaluating the inducibility ratio, in the mono-atrial scenario, subjects p1 and p3 were the most vulnerable, while subjects p2 and p4 were the least vulnerable. In contrast, in the bi-atrial scenario, subject p1 had the fewest number of inducing points, while subjects p2 and p4 were the most vulnerable. Thus, the AVA based on only the LA can differ once the RA is included.

The increased number of reentries observed in the bi-atrial scenarios could be explained by several reasons. Reentries were often anchored around the tricuspid valve ring, the coronary sinus, or around the inter-atrial connections, entering the LA and RA alternately. This observation suggests that the anatomical structures of the RA and the inter-atrial connections are contributing directly to the maintenance of reentries. Regions in the RA such as the pectinate muscles are known to promote reentry formation [6]. According to the leading circle concept [1], functional reentry in the atrium is facilitated by a slower CV and a shorter effective refractory period (ERP). Additionally, it is stated that regarding AF, multiple leading circles are more likely to occur in large hearts. In the matter of slower CV, we observed a greater share of inducing points in the S state (CV 0.8 m/s) than in the M state (CV 1.0 m/s) in most cases (see Figure 2). Furthermore, the RA made up 54.75 % of the surface area in the bi-atrial geometries on average in our cohort of subjects. Thus, bi-atrial models provide more area for potential leading circles, which increases the probability for reentry formation.

We hypothesize a linear increase of the ratio of inducing points and the AF-induced remodelling state. Some of the results from the bi-atrial scenarios support this linear relationship (see Figure 2). For example, subjects p1 and p4 are simultaneously displaying a linear increase in inducibility ratio that corresponds to the EP modelling state. However, the share of inducing points in the M state was higher than in the S state in the cases of subjects p3 and p5, contrary to what was expected. This observation strengthens the argument that for reentry formation, there is an interplay between structural features and EP remodelling. Considering the mono-atrial scenario, if present, the number of inducing points in the S state was always higher than in the M state. Only for subject p3 in the mono-atrial case, a linear relationship between EP state and inducibility ratio was found, in contrast to the biatrial scenario where p1 and p4 showed the same linear relationship. Due to the very few inducing points in the mono-atrial scenario, it is not possible to soundly characterize the relation.

Furthermore, we wanted to evaluate if the RA would affect the inducibility ratio 0f the stimulation points located in the LA. As a result, we compared the increase of inducing points,

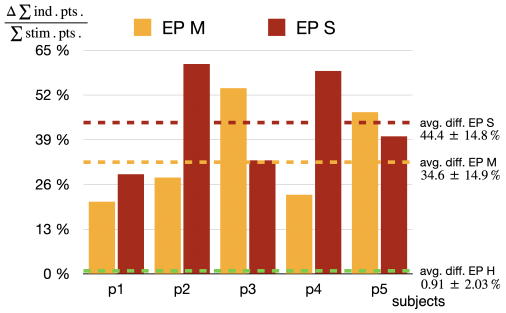

Fig. 3: Percentage point increase of the ratio of inducing points to stimulation points in the LA from the mono-atrial to the bi-atrial scenario for all five subjects.

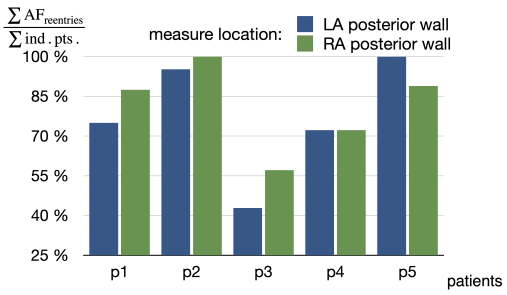

Fig. 4: Ratio of AF classified reentries to inducing points in the S state for all five bi-atrial scenarios.

when stimulated from the LA, between the mono-atrial and bi-atrial scenarios. In every instance, as shown in Figure 3, we observed a noticeable inducibility increase. The additional relative number of inducing points ranged from 21 to 61 %. We found that the RA markedly affected the inducibility ratio even in the mild AF-remodelling scenario, as evidenced by the average increase of 34.6 ± 14.9 % for the M state. While the standard deviation is nearly the same (≈ 15 %,) we also see small average relative variations between the M and S states (34.6 % to 44.4 %). Interestingly, the share of inducing points to stimulation points in the RA was 18.4 ± 6.5 % and 23.9 ± 14.9 % for the M and S states. It seems possible that the RA has more impact on the inducibility ratio of stimulation points in the LA (34.6 ± 14.9 % M, 44.4 ± 14.8 % S) than regarding the ratio of inducing points in the RA itself. Besides that, we observed seemingly random differences in the inducibility ratios of the M and S state. Thus, these findings suggest that the EP state alone cannot explain reentry formation.

We determined the TCL of the induced reentries on the posterior walls of the LA and RA, and we categorized them as AF or AFlut. The ratio of AF classified reentries in the M and S states differ greatly. The average AF classification ratio was 77.1 ± 22.7 % for reentries measured in the LA and 81.2 ± 16.7 % for the RA location in the S state (see Figure 4). Thus, it was more likely to classify a reentry as AF if the TCL

was measured in the RA. In three out of five subjects, this was the case. The increase in AF classification could be attributed to the presence of multiple leading circles and faster TCL in the RA. In terms of the ERP, the chosen EP modelling led to a longer ERP in the RA when compared to the LA [11], however a note of caution is due here since this difference might need further investigation to clarify the influence of the RA's ERP on arrhythmia vulnerability. The differences in the standard deviation of both measurement locations (22.7 % LA, 16.7 % RA), seem to point out the role of the individual atrial geometry. We observed for example that in the S state scenario, there is a noticeable difference in the standard deviation among the subjects, although the EP was the same.

Our study is limited regarding spatially heterogeneous substrate as we did not consider localized fibrotic tissue and its microstructure. In future investigations, it might be possible to model different levels of fibrotic tissue distribution to develop a full picture of the impact of the RA in AVA.

5 Conclusion

Our study suggests an important role for the RA on the results of the AVA. A first evaluation based on the ratio of inducing points to stimulating points can lead to opposite assessments of the subject's vulnerability to reentries when only the LA is considered. It is also possible that only after adding the RA to the LA, reentries may be inducible. Further studies, which take different RA attributes into account, such as the ERP, geometrical aspects like the appendage or heterogeneous substrate might provide important information about where the focus needs to be set when modeling the RA in AVA.

Author Statement

Research funding: This Project has received funding from the European Union's Horizon research and Innovation programme under the Marie Skłodowska-Curie grant agreement No. 860974. Conflict of interest: Authors state no conflict of interest. Informed consent: Informed consent has been obtained from all individuals included in this study. Ethical approval: The research related to human use complies with all the relevant national regulations, institutional policies and was performed in accordance with the tenets of the Helsinki Declaration, and has been approved by the authors' institutional review board or equivalent committee.

References

[1] Allessie, M. A. et al. (1977). Circus movement in rabbit atrial muscle as a mechanism of tachycardia. III. The "leading circle" concept: a new model of circus movement in cardiac tissue without the involvement of an anatomical obstacle. Circ Res 41:9-18

[2] Azzolin, L. et al. (2021). A Reproducible Protocol to Assess Arrhythmia Vulnerability in silico: Pacing at the End of the Effective Refractory Period. Front Physiol 12:656411

[3] Azzolin, L. et al. (2022). AugmentA: Patient-specific Augmented Atrial model Generation Tool. medRixv https://doi.org/10.1101/2022.02.13.22270835

[4] Azzolin, L. et al. (2023). Personalized ablation vs. conventional ablation strategies to terminate atrial fibrillation and prevent recurrence. Europace 25(1):211-222

[5] Boyle, P. et al. (2019). Computationally guided personalized targeted ablation of persistent atrial fibrillation. Nat Biomed Eng 3:870–879

[6] Chen, J. et al. (2000). Dynamics of wavelets and their role in atrial fibrillation in the isolated sheep heart. Cardio Research 48(2):220-232

[7] Cheniti, G. et al. (2018). Atrial Fibrillation Mechanisms and Implications for Catheter Ablation. Front Physiol 9:1458

[8] Courtemanche, M. et al. (1998). Ionic mechanisms underlying human atrial action potential properties: insights from a mathematical model. Am J Physiol 275(1):301-21

[9] Haisaguerre, M. et al. (1998). Spontaneous initiation of atrial fibrillation by ectopic beats originating in the pulmonary veins. N Engl J Med 339(10):659-66

[10] Hocini, M. et al. (2010). Disparate Evolution of Right and Left Atrial Rate During Ablation of Long-Lasting Persistent Atrial Fibrillation. J Am Coll Cardiol 55(10):1007-1016

[11] Krueger, M. W. (2012). Personalized Multi-Scale Modeling of the Atria: Heterogeneities, Fiber Architecture, Hemodialysis and Ablation Therapy. Karlsruhe Trans Biomed Eng 19.

[12] Liu, Y. et al. (2022). Right atrial appendage: an important structure to drive atrial fibrillation. J Interv Card Electrophysiol 65:73–82

[13] Loewe, A. (2016). Modeling human atrial patho-electrophysiology from ion channels to ECG: substrates, pharmacology, vulnerability and P-waves. Karlsruhe Trans Biomed Eng 23.

[14] openCARP consortium et al. (2022). openCARP (v12.0). Karlsruhe Institute of Technology. https://doi.org/10.35097/874

[15] Perino, A. C. et al. (2019). Secular trends in success rate of catheter ablation for atrial fibrillation: The SMASH-AF cohort. Am Heart J 208:110-119

[16] Plank, G. et al. (2021) The openCARP simulation environment for cardiac electrophysiology. Comput Methods Programs Biomed 208:106223

[17] Zaman, J. AB et al. (2022). Future Directions for Mapping Atrial Fibrillation. Arrhythm Electrophysiol Rev 11:e08